encit 2020

ABCM Associação Brasileira de Engenharia e Ciências Mecânicas

18th Brazilian Congress of Thermal Sciences and Engineering
November 16–20, 2020 (Online)

ENC-2020-0300
EFFECTS OF NUMERICAL PARAMETERS IN THE SIMULATION OF SUPERSONIC BLUNT BODY FLOWS

Frederico Bolsoni Oliveira
Instituto Tecnológico de Aeronáutica – DCTA/ITA, 12228-900 – São José dos Campos – SP – Brazil
fredericobolsoni@gmail.com
João Luiz F. Azevedo
Instituto de Aeronáutica e Espaço, DCTA/IAE/ALA, 12228-904 – São José dos Campos – SP – Brazil
joaoluiz.azevedo@gmail.com

Abstract. *The effects induced by mesh geometry and numerical scheme on the solution of supersonic inviscid flows around a blunt body are analyzed, mainly focusing on the structure of the bow shock that commonly arises in such conditions. Four different schemes are considered: Beam and Warming implicit approximate factorization algorithm, the original Steger and Warming flux vector splitting algorithm, the van Leer approach on performing the flux vector splitting and Liou's AUSM$^+$ scheme. Significant changes in the shock structure are observed, mainly due to special properties of the scheme in use and to the influence of the domain transformation procedure. Non-physical behavior is also seen to be prone to arise in such conditions. Freestream subtraction, flux limiting and the explicit addition of artificial dissipation are employed in order to circumvent these problems. Good agreement is achieved with both numerical and experimental results available in the literature.*

Keywords: *Computational Fluid Dynamics, Supersonic Flow, Blunt Body, Bow Shock, Finite Differences*

1. INTRODUCTION

In supersonic aerospace applications, the correct determination of shock wave behavior is of vital importance for the design of high-speed aircraft and spacecraft. One special case of such type of flow is the strong detached shock wave, known as a "bow shock", that develops around solid bodies of specific geometries when immersed in supersonic flowfields. Although sharp leading edge bodies are capable of inducing the fluid to assume a bow shock configuration provided the correct Mach number is in effect, the present paper is mainly interest in bow shocks that arise from the interaction between the fluid and the solid walls of a blunt body. Nowadays, such type of geometry is mainly found on the design of heat shields and nose cones of reentry vehicles. In such cases, the development of a bow shock can be seen as a desired effect, since it elevates the drag coefficient of the body which, in turn, helps it decrease its descent velocity at the cost of a considerable increase on the average wall temperature.

The accurate numerical determination of the detached shock structure is heavily dependent on the numerical scheme used in the discretization of the model equations, as well as on the geometrical properties of the mesh. The present paper investigates these relations by applying four different numerical schemes, in the context of a finite difference method, for the discretization of the compressible Euler equations. This level of formulation is considered to be a reasonable approximation for the behavior of supersonic flows. Here, it is applied to a simple circular two-dimensional blunt body immersed in a supersonic steady flow, as described by Peery and Imlay (1988). Furthermore, the mesh used was purposely designed with the intention of achieving a high curvature along the domain, thus enabling the observation of numerical problems that arise from such condition. The solution is obtained by using an in-house CFD code that implements each one of these numerical methods.

The first scheme used is the implicit Beam and Warming approximate factorization scheme (Beam and Warming, 1978), which uses an implicit Euler time march coupled with a second-order centered scheme for the discretization of the spatial derivatives. Significant reduction in computational cost is achieved by employing an approximate factorization of the ADI (Alternating Direction Implicit) type, which reduces the implicit matrix operator to a block-tridiagonal form and, thus, decreases the computational cost of solving the linear system. Since this is a centered scheme, artificial dissipation must be added to the discretized equations in order to keep the numerical system within stability bounds. Furthermore, it is of interest that the addition of artificial dissipation does not introduce undesirable oscillations to the surroundings of the shock wave. Therefore, Pulliam's nonliner artificial dissipation model (Pulliam, 1986a) is used in the explicit part of the equations, while a simplified version of it is applied to the implicit matrix operator.

The other three numerical schemes follow the Flux Vector Splitting idea. The first one is the Steger and Warming orig-

inal flux vector splitting scheme (Steger and Warming, 1981), coupled with an implicit Euler time march. The main idea behind this family of schemes is to separate the equation flux vectors in two distinct components based on the eigenvalues of the flux Jacobian matrix, which are interpreted as the velocity of the characteristic variables that compose the solution. One of these components is associated with the positive eigenvalues, while the other component is associated with the negative eigenvalues. This enables the usage of one-sided operators since the direction of propagation of information in the solution-field can be respected, which characterizes an upwind scheme.

Steger and Warming's scheme introduces a discontinuity in the derivative of the separated flux vectors in relation to the original eigenvalue when the original eigenvalue changes signs. In the current case, this can be especially problematic in the subsonic region that appears aft the bow shock, near the stagnation point. In order to solve this problem, the van Leer approach for performing the Flux Vector Splitting (van Leer, 1982) is also employed here. Both of these upwind schemes are implemented using first and second order finite difference operators in order to observe the dissipative nature of lowering the order of the scheme.

Finally, we have Liou's Advection Upstream Splitting Method Plus (AUSM$^+$) explicit method (Liou, 1996). This method was originally written using the concept of numerical fluxes and has a distinguishable difference in relation to the other two upwind schemes when it comes to the approach of performing the splitting of the flux vectors. In this case, the flux vector is interpreted as being the sum of the transport of a passive scalar component and a local pressure component. Each one of these components is treated differently during the splitting process. For this scheme, only a first order spacial discretization is considered.

Therefore, the main purpose of the present effort is to address the relevant numerical issues that might influence the accurate calculation of aerospace flows with strong shock waves. In order to have a basis for comparison, the simulation results will be analyzed in relation to the work of Peery and Imlay (1988), Lin (1991) and Holden *et al.* (1988).

2. TWO-DIMENSIONAL NUMERICAL FORMULATION

The two-dimensional form of the Euler equations can be written in conservation-law form and curvilinear coordinates as follows:

$$\frac{\partial \hat{Q}}{\partial \tau} + \frac{\partial \hat{E}}{\partial \xi} + \frac{\partial \hat{F}}{\partial \hat{\eta}} = 0 \tag{1}$$

where $\hat{Q}$ is the vector of conserved variables:

$$\hat{Q} = J^{-1} \begin{Bmatrix} \rho \\ \rho u \\ \rho v \\ e \end{Bmatrix} \tag{2}$$

and $\hat{E}$ and $\hat{F}$ are the flux vectors for the inviscid case:

$$\hat{E} = J^{-1} \begin{Bmatrix} \rho U \\ \rho u U + \xi_x p \\ \rho v U + \xi_y p \\ U(e+p) - \xi_t p \end{Bmatrix}, \quad \hat{F} = J^{-1} \begin{Bmatrix} \rho V \\ \rho u V + \eta_x p \\ \rho v V + \eta_y p \\ V(e+p) - \eta_t p \end{Bmatrix} \tag{3}$$

Here, ρ is the local fluid density, u and v are the Cartesian components of the velocity vector, e is the total energy per unity of volume and p is the static pressure. ξ and η are the main coordinates of the curvilinear domain, τ is the time variable in the new system (made equal to t), and J is the Jacobian of the domain transformation, expressed as:

$$J^{-1} = x_\xi y_\eta - x_\eta y_\xi \tag{4}$$

where the subscript means a partial derivative operator, and the mapping from the Cartesian domain to the curvilinear domain is done in such a way that only discrete unitary variations occur between two adjacent points. The metric terms ξ_t, ξ_x, ξ_y, η_t, η_x ans η_y are calculated from the derivatives of the Cartesian coordinates as shown below:

$$\xi_x = J y_\eta, \quad \xi_y = -J x_\eta, \quad \eta_x = -J y_\eta, \quad \eta_y = J x_\xi, \quad \xi_t = -x_\tau \xi_x - y_\tau \xi_y, \quad \eta_t = -x_\tau \eta_x - y_\tau \eta_y \tag{5}$$

The U and V variables are the contravariant components of the velocity vector. They can be expressed as functions of the metric terms as follows:

$$U = \xi_t + \xi_x u + \xi_y v, \qquad V = \eta_t + \eta_x u + \eta_y v \tag{6}$$

For a thermally and calorically perfect gas, the pressure p can be expressed as:

$$p = (\gamma - 1)\left[e - \frac{1}{2}\rho(u^2 + v^2)\right] \tag{7}$$

It must be said that all variables mentioned so far are used in their nondimensional form by taking a suitable reference value which will always be stated whenever needed. The numerical schemes themselves, in the context of finite differences, assume the same form as described by the authors in Oliveira and Azevedo (2019). Therefore, for the sake of brevity, they are not going to be described here again. The chosen values for the control constants of the artificial dissipation model are $K_2 = 1/4$ and $K_4 = 1/100$.

As will be seen in the next section, multiple numerical problems can arise from the usage of the unmodified version of these schemes in regions that surround strong discontinuities. Therefore, some modifications are presented here in the hope of completely, or partially, solve these problems. The first one of them is a modification to the way that the one-sided second-order finite difference operator is written. The first and second-order, first-difference, backward, discrete one-dimensional operators, Delta and δ^-, can be written, respectively, as:

$$\nabla b_i = \frac{1}{\Delta x}\left(b_i - b_{i-1}\right) \tag{8}$$

$$\delta^- b_i = \frac{1}{2\Delta x}\left(3b_i - 4b_{i-1} + b_{i-2}\right) \tag{9}$$

where b is a dummy variable, i is the index of the current node and Δx is the grid spacing. As shown in Anderson *et al.* (1986), by making ∇b_i explicit in Eq. (9), both operators can be written in a single form, as follows:

$$\delta^- b_i = \nabla b_i + \phi_i \frac{1}{2\Delta x}\left(b_i - 2b_{i-1} + b_{i-2}\right) \tag{10}$$

In Eq. (10), depending on the value of the control variable ϕ_i the backward finite difference operator can either be second-order ($\phi_i = 1$) or first-order ($\phi_i = 0$). Second-order (and above) one-sided operators are known for introducing undesired numerical oscillations near discontinuities in the solution domain. Thus, it is of interest to enable the one-sided operator to decay to first-order whenever such condition is met. In order to ensure a conservative switch between the first and second-order forms of the operator, the ϕ value is allowed to vary spatially and to assume other values besides 0 and 1, enabling a gradual transition between the two forms. When interpreted as a function, ϕ receives the name "flux limiter" and usually takes as argument a parameter that establishes if the current point is near a discontinuity or local oscillation.

In order to enable a finer control over the transition between the two forms of the one-sided operator, Eq.(10) can also be written in a more convenient form:

$$\delta^- b_i = \nabla b_i + \phi_i \frac{1}{2\Delta x}\left(b_i - b_{i-1}\right) - \phi_{i-1}\frac{1}{2\Delta x}\left(b_{i-1} - b_{i-2}\right) \tag{11}$$

or, if the numerical flux notation were to be used, the above equation could be written simply as:

$$\delta^- b_i = \frac{1}{\Delta x}\left(b^-_{i+\frac{1}{2}} - b^-_{i-\frac{1}{2}}\right) \tag{12}$$

with

$$b^-_{i+\frac{1}{2}} = b_i + \frac{1}{2}\phi_i\left(b_i - b_{i-1}\right) = b_i + \frac{\Delta x}{2}\phi_i \nabla b_i \tag{13}$$

$$b^-_{i-\frac{1}{2}} = b_{i-1} + \frac{1}{2}\phi_{i-1}\left(b_{i-1} - b_{i-2}\right) = b_{i-1} + \frac{\Delta x}{2}\phi_{i-1}\nabla b_{i-1} \tag{14}$$

which are essentially one-sided property extrapolations evaluated at the numerical interfaces $i+\frac{1}{2}$ and $i-\frac{1}{2}$. In the present work, the chosen ϕ function is the minmod flux limiter (Roe, 1986):

$$\phi_i = max\left(0, min\left(1, r_i\right)\right) \tag{15}$$

in which r_i is the ratio of consecutive property variations:

$$r_i \equiv \frac{b_i - b_{i-1}}{b_{i+1} - b_i} \tag{16}$$

Notice that, although all equations were shown for the backward one-sided operator, analogous definitions can also be made for the forward operator. These new definitions for the forward and backward operators are used here in the implementation of the second-order Steger and Warming and van Leer schemes. Hence, the limiter function is acting upon the finite difference operator of the flux terms, constraining the size of its stencil. This is a contrast to the Monotone Upstream-Centered Scheme for Conservation Laws (MUSCL) approach, where the limiter acts over the reconstruction of the properties at the numerical cell interface, which is then used to compute the flux terms (van Leer, 1979).

Another problem that must be accounted for is the fact that the discrete Euler equations written in conservation-law form and curvilinear coordinates, as shown in Eq. (1), do not "accept" the freestream state as a possible solution when applied to a non-uniform mesh. This same behavior is also true for the full Navier-Stokes system of equations. This is due to the presence of space-varying metric terms that are computed using finitely accurate finite differences schemes. In order to reduce the influence of this problem over the discrete solution, a freestream subtraction (Pulliam and Steger, 1978) is performed on the calculation of the fluxes of the Euler equations, as follows:

$$\frac{\partial \hat{Q}}{\partial \tau} + \frac{\partial\left(\hat{E} - \hat{E}_\infty\right)}{\partial \xi} + \frac{\partial\left(\hat{F} - \hat{F}_\infty\right)}{\partial \hat{\eta}} = 0 \tag{17}$$

where the subscript ∞ refers to the constant free-stream state. With this modification, it becomes clear that the free-stream state is recovered as a possible discrete solution to the system of equations.

3. DESCRIPTION OF TEST CASE AND BOUNDARY CONDITIONS

The problem consists of a circular body with a $76.2\ mm$ ($3.0\ in.$) diameter, d, immersed in a supersonic flow. The fluid is taken to be atmospheric air with a constant specific heat ratio, γ, of 1.4 and an individual gas constant, R, of $287\ J/(kg\ K)$. The freestream flow is defined by a Mach number, M, of 8.0, a static pressure, p, of $855\ Pa$ and a total temperature, T_t, of $1726\ K$. These conditions are enough to constrain the subsonic region of the flow to a small fluid pocket located between the shock wave and the body surface, around the stagnation point. Hence, the discrete domain can be limited to only a small region that surrounds the upstream part of the body, as long as the flow that crosses its boundaries is fully supersonic. If this condition is met, then the subsonic wake that develops downstream will not affect the results obtained for this isolated supersonic region.

One possible way of defining the domain is as shown in Fig. 1, where the origin is located at the body geometrical center, with the x axis pointing towards the right direction and the y axis pointing upwards. The outer boundary is an arc of a circle with a diameter of $3.5d$. A structured mesh is, then, created using 100×100 nodes distributed with a slight bias towards the wall region. One should notice that the mesh lines are purposely created such that they do not follow the shock surface.

The right boundary is taken to be a solid wall, the left boundary is the supersonic free-stream itself and the upper and lower boundaries are supersonic outflow regions, whose properties are calculated using first-order extrapolation. In order to make sure that the solution converges when performing the time-march, if a subsonic condition is identified at the supersonic outflow boundaries at any given moment, then a static pressure equal to $p/3$ is enforced in order to recover the supersonic state. Here, the solution is considered to be converged when the residue associated with the continuity equation decreases by 11 orders of magnitude or more, unless otherwise stated.

4. RESULTS AND DISCUSSION

Contour plots of the converged Mach number distribution in the steady state flow are shown in Figs. 2, 3 and 4 for the first-order Steger and Warming, van Leer and AUSM$^+$ upwind schemes, respectively, without performing the freestream subtraction. As it can be seen, although all three schemes were able to achieve similar results in terms of the macro properties of the flow, such as overall bow shock location and Mach number spatial distribution, there are a few inconsistencies of numerical nature that surround the domain symmetry line (x axis), in the region near the shock. In all three cases, there are nonphysical oscillations that appear in the upstream region of the bow shock, where an undisturbed

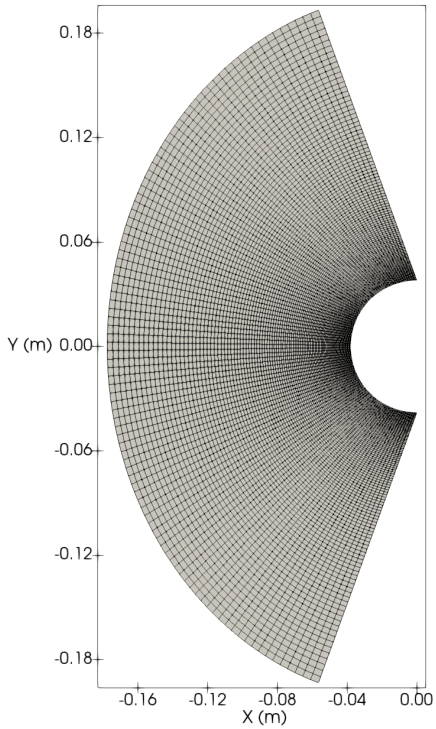

Figure 1. View of the computational domain defined for the simulation as well as the structured mesh used (100x100 nodes). Coordinate units are in meters.

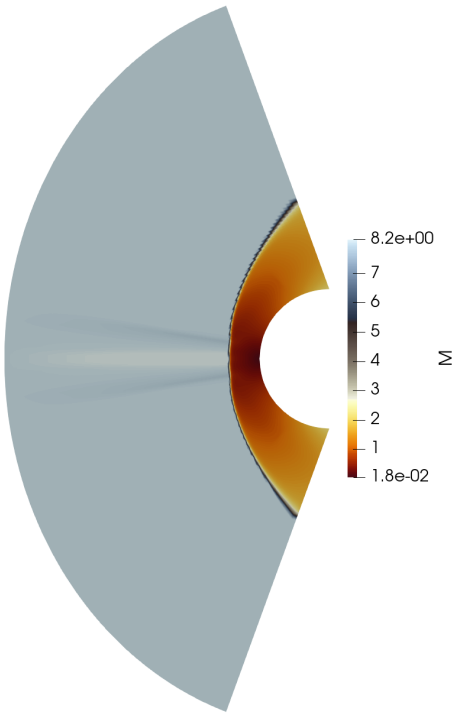

Figure 2. Calculated Mach number distribution for the inviscid blunt body flow using the first-order Steger and Warming upwind scheme without using freestream subtraction.

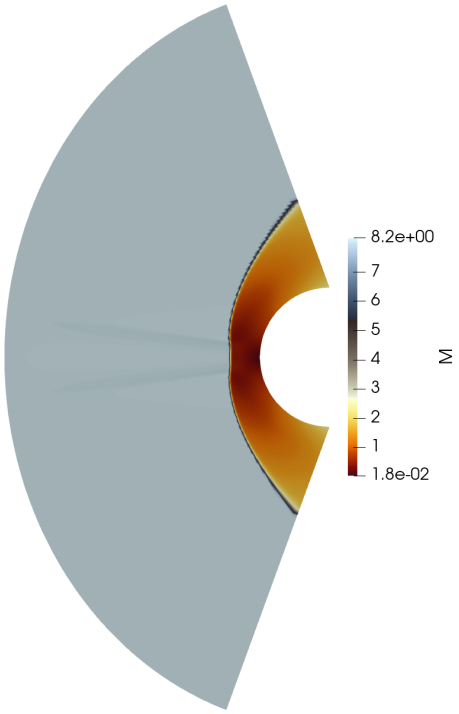

Figure 3. Calculated Mach number distribution for the inviscid blunt body flow using the first-order van Leer upwind scheme without using freestream subtraction.

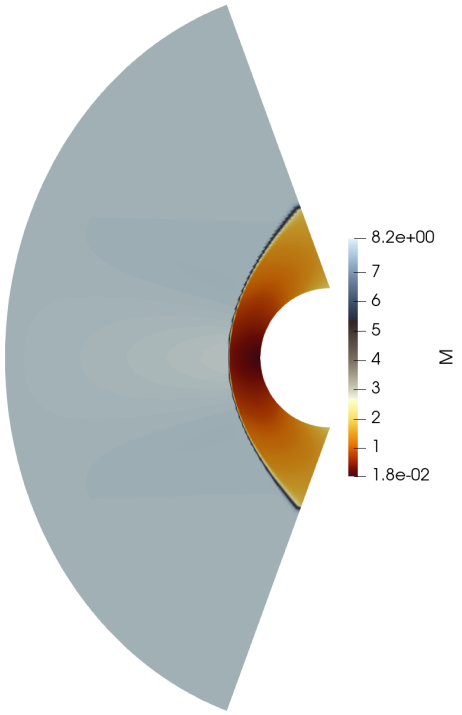

Figure 4. Calculated Mach number distribution for the inviscid blunt body flow using the first-order AUSM$^+$ upwind scheme without using freestream subtraction.

freestream state was expected. This numerical problem is more apparent in the case of the first-order Steger and Warming scheme, as can be seen in Fig. 2.

A better view of these numerical oscillations can be achieved if a flow property, such as the Mach number, is plotted along a vertical line located in the upstream region of the shock. The chosen vertical line is located at $x = -0.07\,m$, and

goes from $y = -0.03\,m$ to $y = +0.03\,m$. Mach number values obtained for each one of the three first-order schemes are plotted along the vertical line in Fig. 5. As it can be seen, a considerable deviation from the analytical constant freestream state of $M_\infty = 8.0$ is observed in all three schemes. The most critical case is seen in the first-order Steger and Warming scheme, whose Mach number values can reach a difference of up to 4.4% in relation to the analytical freestream solution-state, followed by 1.7% for the AUSM$^+$ and 1.4% for the van Leer scheme. In locations far enough from the centerline of the domain, not pictured in Fig. 5, the freestream state is recovered by all three first-order upwind schemes.

An interesting observation that can be made based on Fig. 5 is that even though the oscillations themselves are of pure numerical nature, their behavior still follows the expected relative performance between each one of the schemes. Both Steger and Warming and van Leer schemes, being based on similar approaches for performing the flux vector splitting, produce oscillations of similar geometry. The latter scheme, however, produce oscillations of smaller magnitude when compared to the former one. This follows the trend already discussed in the literature (Anderson *et al.*, 1986), in which the van Leer scheme is capable of achieving better results than the Steger and Warming scheme in general transonic flows. On the other hand, while the oscillations produced by both Steger and Warming and van Leer schemes have well-defined edges, the ones produced by the AUSM$^+$ scheme are completely smooth.

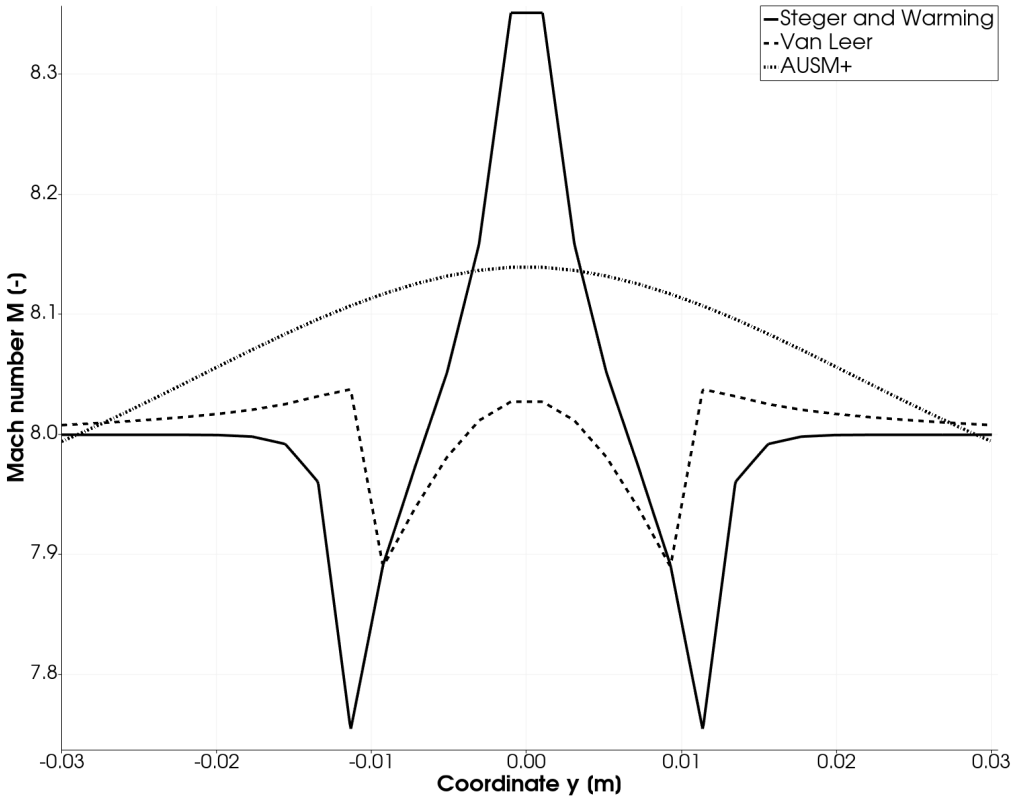

Figure 5. Calculated Mach number along a vertical line located in the upstream region of the shock ($x = -0.07\,m$) for three different first-order upwind schemes. A constant freestream state of $M_\infty = 8.0$ is expected.

As discussed by Pulliam (1986b), the correct capture of the freestream state when using discrete general curvilinear coordinates requires that the invariants of the domain transformation be true even in discrete form. However, this is, in general, not the case. These invariants are partial differential equations themselves, which are equal to zero and primarily dependent on the metric terms. Inaccuracies and inconsistencies in the discrete treatment of the metric terms are the main reasons for the invariants to not be equal to zero. Therefore, the discrete metric terms are most likely the major source of these oscillations. The AUSM$^+$ scheme, as employed here, utilizes a continuous well-behaved polynomial function to reconstruct the metric terms that accompany the pressure related components of the separated flux vectors (Oliveira and Azevedo, 2019). Therefore, this same continuous property is also seen in the behavior of the oscillations introduced by the AUSM$^+$ scheme, a contrast to the ones introduced by both the Steger and Warming and van Leer schemes. Since the metric terms are functions of the mesh geometry, it is expected that this problem becomes more apparent with the increase in mesh curvature. This leads to higher gradients in the metric terms, which increase the error associated with the invariants of the domain transformation.

In order to solve the oscillation problem, it was seen that by simply performing the freestream subtraction, a considerable reduction in the magnitude of the oscillations was achieved. For the Steger and Warming scheme, a reduction of at least 6 orders of magnitude was observed and, from a practical point of view, made the discrete values behave as expected

from the analytical solution for this region. Similar improvements in the quality of the solution were also observed for the van Leer and AUSM$^+$ schemes when performing the freestream subtraction. Therefore, for now on, all schemes analyzed here are using the freestream subtraction.

Another problem, also seen in Fig. 3, is the deformation that the first-order van Leer scheme induces over the bow shock surface in the region that surrounds the symmetry line. Apparently, this deformation also has the same origin as the freestream oscillations, since it was observed that it completely disappears once the freestream subtraction is in place. Figure 6 shows the Mach number contours for the first-order van Leer scheme with freestream subtraction. One can clearly see that no oscillations are present in the freestream region of the flow, as well as no significant deformations exist in the shock surface, as was originally intended.

For the second-order schemes, however, a different set of problems arise. First, both upwind schemes constructed with pure second-order operators, promptly diverge when performing the time march. When looking at the pseudo-transient solution, it is clear that the divergence comes from induced numerical oscillations that appear parallel to the surface of the shock. These oscillations quickly increase in magnitude, leading the solution to eventually diverge. This chaotic behavior can be attributed to the lack of sufficient artificial dissipation introduced by the schemes. One possible way of solving this problem is to simply explicitly add artificial dissipation to the discrete equations, such as the Pulliam non-linear artificial dissipation model. Another possible way of increasing the amount of artificial dissipation is to utilize first-order one-sided operators in the region that surround the shock wave. This can be achieved by using a flux limiter, as shown in the previous section. It was seen that either one of these approaches was able to fully stabilize the second-order upwind schemes, enabling them to reach a steady state regime. However, this was not possible without introducing some drawbacks.

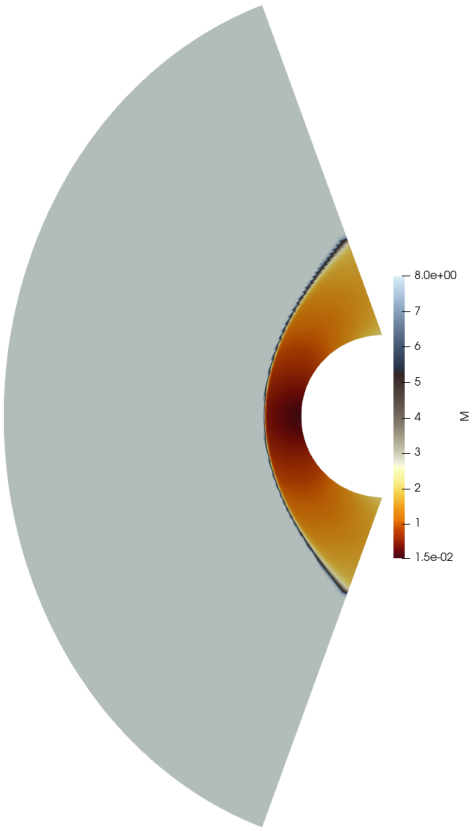

Figure 6. Calculated Mach number distribution for the inviscid blunt body flow using the first-order van Leer upwind scheme with freestream subtraction.

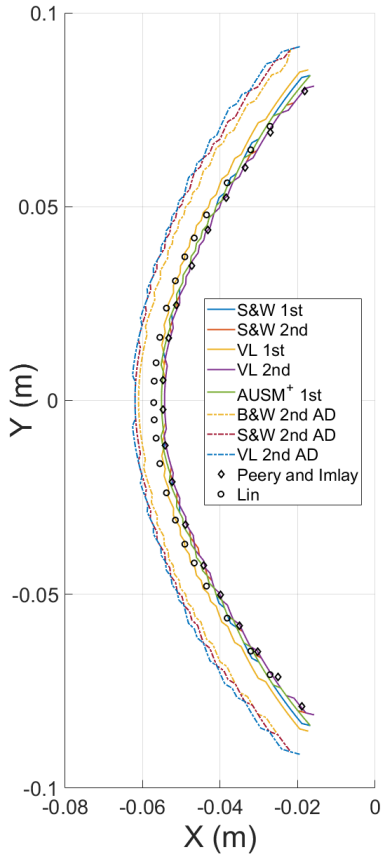

Figure 7. Approximate shock wave location obtained by the first and second-order schemes, with and without explicit artificial dissipation (AD). Results from Peery and Imlay (1988) and Lin (1991) are included for comparison.

Figure 7 shows the approximate shock wave location obtained by using the first and second-order schemes. This location is taken to be composed by the set of node coordinates in which the local Mach number has a measurable deviation from the freestream state. The results for the second-order upwind schemes are obtained by either using the minmod limiter or by explicitly adding the Pulliam artificial dissipation model. Numerical experiments performed by Peery and Imlay (1988) and Lin (1991), using modified versions of Roe's scheme to solve the full Navier-Stokes equations,

are also added for comparison. As clearly shown in the figure, there is significant aliasing in the shock surfaces obtained in the present work when compared to the results from the other efforts. This is due to the misalignment between the shock surface and the mesh lines present here. In Peery and Imlay (1988) and Lin (1991), however, the mesh was built in such a way that a good alignment is obtained between the shock surface and the mesh lines. Furthermore, other numerical tools were also used in order to smooth out this effect. Therefore, they do not suffer from this problem.

Another property, seen in Fig. 7, is that the solutions can be organized into two different groups based on the predicted shock wave location. The first one is composed by the methods that do not use explicit artificial dissipation, while the other one is composed by those that do use it. Notice that, when it comes to the location of the shockwave at the centerline of the domain, there is a significant gap between these two groups. It seems that the artificial dissipation model is moving the shock wave in the upstream direction. Although not shown here, when the original Beam and Warming artificial dissipation model (Beam and Warming, 1978) is used instead, a similar behavior is also displayed. Modifying the model constants does not change this behavior in any meaningful way. The authors are still investigating the reason for this numerical phenomenon.

One can further observe that the differences among the calculated shock wave locations increase at regions that are further away from the domain centerline, when comparing the solutions that are part of the same group. The different grouping patterns, though, are still well defined in these regions. When it comes to the quality of the solutions, it is clear that the schemes that do not use explicit artificial dissipation show good agreement with the data from Peery and Imlay (1988). This is especially true for the second-order upwind schemes, which are capable of reproducing the data really closely. The results from Lin (1991), however, are located slightly upstream in relation to the first solution group. This difference in the results is constrained to a small region surrounding the centerline. This might be due to a not fully suppressed carbuncle phenomenon (Peery and Imlay, 1988), or due to inaccuracies introduced by the process of extracting the data from the original paper. Another possibility is that the dissipation model that is used in Lin's work, which has a term similar to the one used in the Pulliam model, is also translating the shock upstream.

Although the usage of a limiter to stabilize the second-order upwind schemes achieved better results than the explicit addition of artificial dissipation, a new disadvantage gets introduced to the scheme. Now, the residue of the solution is unable to decrease 11 orders of magnitude, as obtained with the other schemes. Instead, a reduction of only 3 to 4 orders of magnitude was seen to be possible. The authors believe that the usage of a more robust limiter might at least mitigate this problem.

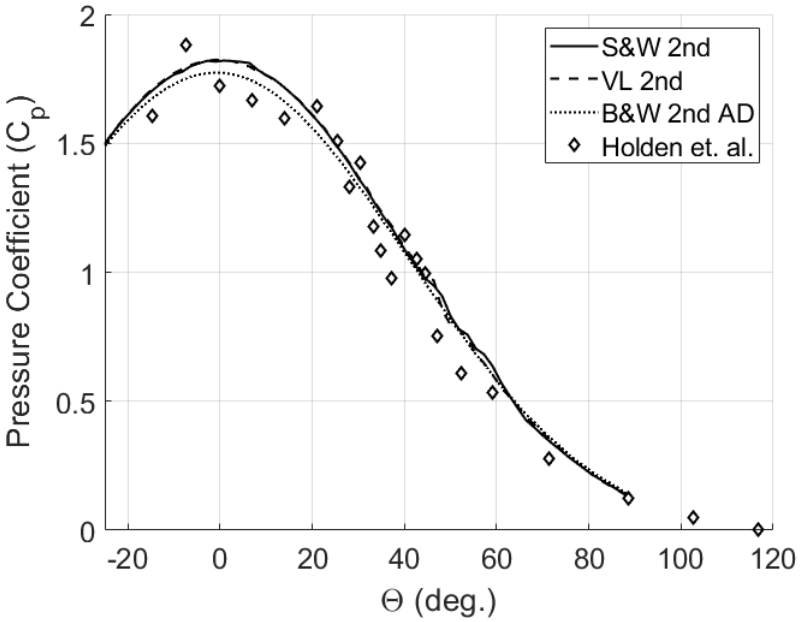

Figure 8. Pressure coefficient (C_p) distribution along the surface of the cylinder. The θ angle is measured from the center of the cylinder in relation to the centerline of the domain, in the counterclockwise direction. Experimental data from Holden *et al.* (1988) is included for comparison.

In Fig. 8, pressure coefficient (C_p) distribution along the cylinder surface is shown for the second-order schemes. The surface location is identified by the θ angle, which is measured from the center of the cylinder in relation to the centerline of the domain, in the counterclockwise direction. Upwind results are obtained only using a limiter, without introducing extra explicit artificial dissipation. Experimental results from Holden *et al.* (1988) are also shown for comparison. As it can be seen, good agreement with experimental data is obtained for all schemes even though an inviscid formulation

is used. Both second-order Steger and Warming and van Leer schemes obtained very similar results, with exception to the region between 40 and 60 deg. In this region, oscillations can be observed in the solution obtained with the Steger and Warming scheme. That is the exact region where the flow passes through a sonic line and, as such, the Steger and Warming scheme induces the surge of small glitches in the solution (Anderson *et al.*, 1986). The results obtained with the Beam and Warming scheme are really close to the others for θ angles above 25 deg., even though its shock wave is located significantly upstream. Close to the centerline, which is where the subsonic flow pocket is located, there is a measurable deviation from the other results. Exactly at the centerline, for example, the calculated C_p is approximately 2.7% lower than the value obtained by the second-order upwind schemes. Due to the dispersion present in the experimental data at this region, it is difficult to assess the relative performance of the schemes in relation to the quality of the C_p values at low θ angles.

5. CONCLUDING REMARKS

It is interesting that a two-dimensional blunt body flow consists in a very simple geometry, which, then, could lead one to believe that numerically capturing such flow would be a trivial task. The present results are showing that the correct definition of the supersonic inviscid flow that surrounds a circular blunt body can impose a significant challenge to multiple numerical schemes. Care must be exerted by the CFD user in order to avoid adding non-physical structures to the calculated properties. In the context of equations written in general curvilinear coordinates and discretized using finite differences, freestream subtraction is seen to be of utmost importance to the correct capture of the shock wave. Its usage eliminates structures of numerical nature in the upstream region of the flow and enables a better definition of the shock profile. The presence of these structures is related to the metric terms of the domain transformation, which are functions of the mesh geometry itself.

Second-order upwind schemes are, in the case treated here, unstable. The usage of a limiter or the explicit addition of artificial dissipation are seen to be capable of stabilizing the solution process. Nevertheless, results obtained using explicit addition of artificial dissipation models translate the location of the shock in the upstream direction. No clear reason for this behavior has been found yet and it is currently being investigated by the authors. In summary, for the schemes in which such numerical spurious constructions are adequately controlled, or absent, good agreement has been found between the numerical results and the data available in the literature.

6. ACKNOWLEDGEMENTS

The authors wish to express their gratitude to Coordenação de Aperfeiçoamento de Pessoal de Nível Superior, CAPES, which has supported the present research through a graduate scholarship for the first author. The authors also gratefully acknowledge the support for the present research provided by Conselho Nacional de Desenvolvimento Científico e Tecnológico, CNPq, under the Research Grant No. 309985/2013-7. The work is further supported by Fundação de Amparo à Pesquisa do Estado de São Paulo, FAPESP, under the Research Grant No. 2013/07375-0.

7. REFERENCES

Anderson, W.K., Thomas, J.L. and van Leer, B., 1986. "Comparison of finite volume flux vector splittings for the Euler equations". *AIAA Journal*, Vol. 24, No. 9, pp. 1453–1460.

Beam, R.M. and Warming, R.F., 1978. "An implicit factored scheme for the compressible Navier-Stokes equations". *AIAA Journal*, Vol. 16, No. 4, pp. 393–402.

Holden, M.S., Moselle, J.R. and Lee, J., 1988. "Studies of aerothermal loads generated in regions of shock/shock interaction in hypersonic flow". AIAA Paper No. 88-0477, *26th Aerospace Sciences Meeting*, Reno, NV, USA.

Lin, H.C., 1991. "Dissipation additions to flux-difference splitting". AIAA Paper No. 91-1544, *10th AIAA Computational Fluid Dynamics Conference*, Honolulu, HI, USA.

Liou, M.S., 1996. "A sequel to AUSM: AUSM$^+$". *Journal of Computational Physics*, Vol. 129, pp. 364–382.

Oliveira, F.B. and Azevedo, J.L.F., 2019. "Effects of numerical parameters and artificial dissipation in the simulation of inviscid nozzle flows". COBEM Paper No. 2019-1227, *25th ABCM International Congress of Mechanical Engineering*, Uberlândia, Brazil.

Peery, K.M. and Imlay, S.T., 1988. "Blunt-body flow simulations". AIAA Paper No. 88-2904, *AIAA/SAE/ASME/ASEE 24th Joint Propulsion Conference*, Boston, MA, USA.

Pulliam, T.H., 1986a. "Artificial dissipation models for the Euler equations". *AIAA Journal*, Vol. 24, No. 12, pp. 1931–1940.

Pulliam, T.H., 1986b. "Solution methods in computational fluid dynamics". Notes for the von Kármán Institute for Fluid Dynamics Lecture Series, von Kárman Institute, Rhode-St-Genese, Belgium.

Pulliam, T.H. and Steger, J.L., 1978. "On implicit finite-difference simulations of three dimensional flow". AIAA Paper No. 78-10, *16th AIAA Aerospace Sciences Meeting*, Huntsville, AL, USA.

Roe, P.L., 1986. "Characteristic-based schemes for the Euler equations". *Annual Review of Fluid Mechanics*, Vol. 18, pp. 337–365.

Steger, J.L. and Warming, R.F., 1981. "Flux vector splitting of the inviscid gasdynamic equations with application to finite-difference methods". *Journal of Computational Physics*, Vol. 40, pp. 263–293.

van Leer, B., 1979. "Towards the ultimate conservative difference scheme V: A second-order sequel to Gudonov's method". *Journal of Computational Physics*, Vol. 32, pp. 101–136.

van Leer, B., 1982. "Flux-vector splitting for the Euler equations". *Lecture Notes in Physics*, Vol. 170, Springer-Verlag, pp. 507–512.

8. RESPONSIBILITY NOTICE

The authors are solely responsible for the printed material included in this paper.